Journal of Coordination Chemistry

ISSN: 0095-8972 (Print) 1029-0389 (Online) Journal homepage: https://www.tandfonline.com/loi/gcoo20

Synthesis, spectroscopic characterization, DFT calculations, and antimicrobial activities of N-arylsalicylaldiminate derivatives of diorganotin(IV)

Raj Kumar Dubey, Avadhesh Pratap Singh, Nitesh Jaiswal, Divya Pratap Singh, Meenakshi, Ajeet Kumar Kushwaha, Manoj Kumar & Afreen Anjum

To cite this article: Raj Kumar Dubey, Avadhesh Pratap Singh, Nitesh Jaiswal, Divya Pratap Singh, Meenakshi, Ajeet Kumar Kushwaha, Manoj Kumar & Afreen Anjum (2019) Synthesis, spectroscopic characterization, DFT calculations, and antimicrobial activities of N-arylsalicylaldiminate derivatives of diorganotin(IV), Journal of Coordination Chemistry, 72:19-21, 3371-3384, DOI: 10.1080/00958972.2019.1689563

To link to this article: https://doi.org/10.1080/00958972.2019.1689563

JOURNAL OF COORDINATION CHEMISTRY
2019, VOL. 72, NOS. 19–21, 3371–3384
https://doi.org/10.1080/00958972.2019.1689563

Synthesis, spectroscopic characterization, DFT calculations, and antimicrobial activities of N-arylsalicylaldiminate derivatives of diorganotin(IV)

Raj Kumar Dubey[a†], Avadhesh Pratap Singh[a,b], Nitesh Jaiswal[a,c], Divya Pratap Singh[d], Meenakshi[a], Ajeet Kumar Kushwaha[a], Manoj Kumar[a] and Afreen Anjum[a]

[a]Synthetic Inorganic and Metallo-Organic Research Laboratory, Department of Chemistry, University of Allahabad, Allahabad, India; [b]Department of Chemistry, Kamla Nehru Institute of Physical and Social Sciences, Sultanpur, India; [c]Department of Chemistry, Prof. Rajendra Singh (Rajju Bhaiya) Institute of Physical Sciences for Study & Research, VBS Purvanchal University, Jaunpur, India; [d]Department of Chemistry, Rajkiya Engineering College, Deogaon, Azamgarh, India

ABSTRACT

Equimolar reaction of di-*n*-butyltin(IV) complexes of bidentate Schiff bases of the type [$(n\text{-Bu})_2$Sn(sb)Cl] with sodium salt of mono-functional bidentate ligands in THF-benzene solution afforded structurally interesting complexes of the type [$(n\text{-Bu})_2$Sn(sb)(L)] (**1**–**6**) [where sbH = Schiff bases: N-salicylidene-2-aminopyridine (sapH) **I**, N-salicylidene-2-methylaminobenzene (*o*-smabH) **II**, and N-salicylidene-4-methylaminobenzene (*p*-smabH) **III**; LH = mono-functional bidentate ligands, acetylacetone (acacH), ethanolamine (eaH)]. All these colored solid complexes were soluble in common organic solvents and characterized by elemental (C, H, N, and Sn) analysis, spectroscopic techniques [IR, (^{1}H, ^{13}C, and ^{119}Sn) NMR] and mass spectrometry. Thermogravimetric analysis of complexes shows thermal behavior and stability of complexes. Computational studies of the synthesized Schiff bases and their organotin(IV) complexes were carried out using DFT which validate the structure of complexes proposed on the basis of spectroscopic data. The mixed-ligand complexes of diorganotin(IV) and Schiff bases were screened for their antibacterial and antifungal activities.

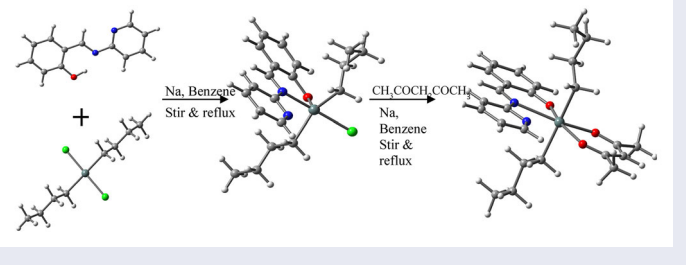

ARTICLE HISTORY

Received 14 August 2018
Accepted 19 October 2019

KEYWORDS

Schiff bases; organotin(IV) complexes; 119Sn NMR; DFT; biological activity

CONTACT Avadhesh Pratap Singh avadheshchem@ymail.com; dpsingh_011@yahoo.co.in Department of Chemistry, Kamla Nehru Institute of Physical and Social Sciences, Sultanpur-228118, India
†Deceased November 2018

Supplemental data for this article can be accessed here.

1. Introduction

Metal complexes are versatile molecules due to the inherent characteristics of both metal center and ligand, providing for a wide range of applications. The N-, O-, and S-donor ligands categorized under Schiff bases are playing a vital role in reconnoitering new dimensions of coordination chemistry of tin complexes [1–3]. Tin complexes of Schiff base derivatives are getting momentous attention due to its important applications. Instead of being toxic in bulk, tin complexes at molecular level in trace amounts play a very crucial role in biological systems [4–8]. Recently, the chemistry of organotin(IV) complexes of Schiff bases has also shown significant potential for their antitumor, antimicrobial, antinematicidal, antiinsecticidal, and antiinflammatory activities [9, 10]. Beside this, organotin(IV) compounds have been paid reasonable attention currently due to their biocompatibility with DNA and cells at molecular level [11–15].

In view of the structural variety and the potential applications of organotin compounds in medicinal chemistry and biotechnology, it was considered worthwhile to synthesize the mixed-ligand organotin(IV) complexes with salicylaldehyde-derived Schiff bases to investigate the interaction of these compounds with biological systems. In continuation of our studies on synthesis and characterization of tin(IV) and organotin(IV) complexes, we have recently reported the synthesis, structural, and DNA cleavage properties of a series of diorganotin(IV) complexes [16]. Furthermore, studies on organotin(IV) derivatives containing O,N- and O,O-bidentate ligands having possibility of structural diversity and our pioneering work [17, 18] on tin(IV) and organotin(IV) chemistry has earlier focused mainly on the use of N-arylsalicylaldimine Schiff bases as effective and versatile coordinating ligands. This encouraged us to synthesize mixed-ligand complexes of organotin(IV), which may lead to complexes with different properties.

We have selected the N-arylsalicylaldimine Schiff bases and mono-functional bidentate ligands as the suitable chelating unit [19], which result in attractive molecular architecture with dibutylorganotin(IV) chloride through their versatile bonding nature either η^1 or η^2. We report in this paper for the first time the reaction of Schiff base complexes of di-*n*-butyltin(IV) dichloride of the type [(*n*-Bu)$_2$Sn(sb)Cl] containing chloride as reactive species with acetyl acetone (acacH) and ethanolamine (eaH) and resulted complexes were characterized by various spectroscopic techniques. The computational calculation of complexes as well as ligands was also performed. The synthesized mixed-ligand complexes of diorganotin(IV) and Schiff bases were investigated for their subsequent applications in antibacterial and antifungal activities.

2. Experimental

2.1. Materials and physical measurements

All the chemicals used throughout the present course of experimental work were of AR grade. The solvents used were of reagent grade and purified by standard procedures [20]. Acetylacetone and ethanolamine from Merck were distilled prior to use. Di-*n*-butyltin(IV) dichloride, *o*-toluidine, 2-aminopyridine, and salicylaldehyde from Sigma Aldrich were used as they were received. Tin was estimated gravimetrically [21] as SnO_2, after decomposition with HNO_3. A Euro-E 3000 elemental analyzer was used for elemental

analysis. A Perkin-Elmer 100 FT-IR spectrometer (4000–400 cm^{-1}) was used for recording infrared spectra of complexes. ^{1}H and ^{13}C NMR spectra were recorded on a Bruker DRX-300 spectrometer and chemical shifts were given in ppm relative to Me_4Si for carbon and hydrogen in $CDCl_3$. ^{119}Sn NMR spectra were recorded on a JEOL-500 spectrometer and chemical shifts were given in ppm relative to Me_4Sn in $CDCl_3$. ESI-MS spectra were recorded on Agilent 6520 Q-Tof LCMS, MS/MS spectrometers, respectively. A TGA Q500 instrument was used for thermal analysis of complexes. The DFT calculations for geometry optimization were performed with the help of Gaussian 09 quantum mechanical software, employing a widely used hybrid exchange-correlation functional B3LYP and LANL2DZ basis set to describe all the atoms including Sn metal [21].

2.2. In vitro microbial activity measurement

The antimicrobial test of the Schiff bases and mixed-ligand organotin(IV) complexes (**1**–**6**) was carried out using the agar well diffusion method [22]. Complexes **1**–**6** were tested for the inhibitory effect on growth of different gram bacteria such as *Escherichia coli*, *Pseudomonas aeruginosa* (as Gram-negative bacteria), and *Staphylococcus aureus*, *Staphylococcus epidermidis* (as Gram-positive bacteria). The concentration of reference, ligands, and diorganotin(IV) complexes is 1 mg/mL in DMSO for antibacterial studies. The antifungal activity of the synthesized organotin complexes has been tested against *Aspergillus niger*, *Candida albicans*, *Trichophyton rubrum*, and *Microsporum*. The concentration of reference, ligands and, diorganotin(IV) complexes is 100 μg/mL in DMSO for antifungal studies. Nutrient agar media was prepared and autoclaved. Each bacterial/fungal species was inoculated by pour plate method (i.e. 20 μL/15 cm^3 of media) to get a confluent growth. The media were poured in sterile and autoclaved petriplates and allowed to solidify for 1 h. When the media were solidified wells were made in it and marked as 1 (positive control i.e. tertracycline with conc. 50 μL/cm^3), 2 (negative control i.e. distilled water), 3 and 4 (different extracts with conc. 400 mg/cm^3). 30 μL of each sample (i.e. controls and extracts) was loaded in respective wells. The plates were then incubated at 37 °C overnight. After 24 h, the antibacterial/antifungal activities were expressed in terms of the diameter of the zone of inhibition (in mm) of each bacterial species by different samples.

2.3. Synthesis of Schiff bases

The Schiff base ligands (L**H**) were synthesized according to the procedure described in our earlier publications [10, 18]. A solution of salicylaldehyde (1.54 g, 12.61 mmol) in methanol was added to a methanolic solution of 2-aminopridine (1.18 g, 12.61 mmol) with constant stirring. The resulting reaction mixture was refluxed for 4 h and left overnight. Yellow crystals were obtained which were recrystallized from methanol.

2.4. Synthesis of complexes

The precursor of the reaction, [*n*-Bu_2Sn(sb)Cl], was synthesized by the interactions of di-*n*-butyltin(IV) dichloride with sodium salts of Schiff bases in equimolar ratio. The reaction of [*n*-Bu_2Sn(sb)Cl] with mono-functional bidentate ligands (L**H**) in equimolar

ratio afforded structurally interesting mixed-ligand complexes of type [(*n*-Bu)$_2$Sn(sb)(L)] (**1**–**6**). Similar procedure was used for the preparation of **1**–**6**, therefore, general preparative details are given for **1**: To a THF (∼20 mL) solution of [*n*-Bu$_2$Sn(sap)Cl] (1.92 g, 4.12 mmol), sodium salt of mono-functional bidentate ligands [prepared by the reaction of equimolar amounts of sodium metal (0.094 g, 4.12 mmol) and a monofunctional bidentate ligand, acetyacetone (0.412 g, 4.12 mmol) in THF (∼30 mL)] in 1:1 molar ratios was added dropwise with constant stirring. The reaction mixture was refluxed for ∼5 h. The precipitated NaCl was removed by filtration and the solvent was removed by distillation. The solid products were dried under reduced pressure and recrystallized from a mixture of THF/n-hexane (20:80) at −20 °C.

2.4.1. [(n-Bu)$_2$Sn(sap)(acac)] (1)

Yield: 69%, brown solid, m.p.135–138 °C, MW: 529.26; Elem. Anal. for $C_{25}H_{36}N_2O_3Sn$, Calcd: C, 56.82; H, 6.96; N, 5.41; Sn, 22.53. Found: C, 56.52; H, 6.83; N, 5.12; Sn, 22.34%. ^{1}H NMR ($CDCl_3$), δ (ppm): 9.69 (1H, s, CH = N); 8.09 (1H, d, Py–H); 6.72–7.81 (7H, m, Ar, Py); 1.28–1.61 (12H, m, Sn–$(CH_2)_3$–); 0.93 (6H, t, CH_3); 3.51 (3H, s, O=C–CH_3); 2.36 (3H, br, –O–C–CH_3); 5.39 (1H, =CH–). ^{13}C NMR ($CDCl_3$) δ (ppm): 159.2 (1C, CO); 157.9 (s, CN); 148.7, 135.2, 134.9, 132.5, 131.9, 130.1, 125.2, 120.5, 115.9, 114.7 (10C, Ar–C, Py–C); 180.6 (–C=O); 189.9 (–C–O); 81.6 (1C, –CH=); 25.6, 16.9 (2C, –CH_3); 32.8, 26.3, 21.9, 13.8 (8C, Sn–Bu^n). ^{119}Sn NMR ($CDCl_3$) δ (ppm): −244.5. IR (cm^{-1}): 1610 *v*(C=N), 1579, 1525 *v*(C=O); 683, 656 *v*(Sn–C); 575, 552, 533 *v*(Sn–O); 429 *v*(Sn–N). ESI-MS (*m/z*): 531.1.

2.4.2. [(n-Bu)$_2$Sn(sap)(ea)] (2)

Yield: 76%, brown solid, m.p. 120–121 °C, MW: 490.23; Elem. Anal. for $C_{22}H_{33}N_3O_2Sn$, Calcd: C, 53.90; H, 6.79; N, 8.57; Sn, 24.22. Found: C, 53.69; H, 6.48; N, 8.45; Sn, 24.10%. ^{1}H NMR ($CDCl_3$) δ (ppm): 9.89 (1H, s, CH = N); 7.99 (1H, d, Py–H); 7.68–6.64 (7H, m, Ar, Py); 1.26–1.78 (12H, m, Sn–$(CH_2)_3$–); 0.85 (6H, t, CH_3); 3.66 (2H, t, O–CH_2–); 2.66 (2H,br, N–CH_2); 2.52 (1H, NH_2). ^{13}C NMR ($CDCl_3$) δ (ppm): 157.8 (s, CO); 156.7 (s, CN); 147.4, 137.9, 136.9, 134.4, 132.4, 130.2, 128.3, 126.3, 121.1, 115.6 (10C, Ar–C, Py–C); 49.0 (1C, –O–CH_2); 31.8 (1C, –N–CH_2); 27.1, 24.1, 21.5, 13.0 (8C, Sn–Bu^n). ^{119}Sn NMR ($CDCl_3$) δ (ppm): −247.0. IR (cm^{-1}): 1614 *v*(C=N); 677, 640 *v*(Sn–C); 525, 552 *v*(Sn–O); 450, 435 *v*(Sn–N). ESI-MS (*m/z*): 490.1.

2.4.3. [(n-Bu)$_2$Sn(o-smab)(acac)] (3)

Yield: 69%, brown solid, m.p.127–129 °C, MW: 544.31; Elem. Anal. for $C_{27}H_{39}NO_3Sn$, Calcd: C, 59.58; H, 7.22; N, 2.57; Sn, 21.81. Found: C, 59.38; H, 7.06; N, 2.36; Sn, 21.57%. ^{1}H NMR ($CDCl_3$) δ (ppm): 9.49 (1H, s, CH=N); 8.81–7.72 (8H, m, Ar–H); 1.52–1.31 (12H, m, Sn–$(CH_2)_3$–); 0.90 (6H, t, CH_3); 2.21 (3H, s, Ar–CH_3); 1.51 (3H, s, O=C–CH_3); 2.26 (3H, s, –O–C–CH_3); 5.39 (1H, =CH–). ^{13}C NMR ($CDCl_3$) δ (ppm): 163.2 (s, CO); 159.5 (s, CN); 147.8, 141.6, 139.2, 136.2, 133.9, 130.2, 128.5, 124.8, 119.9, 115.1, 113.5 (11C, Ar–C); 182.1 (–C = O); 190.9 (–C–O); 80.1 (1C, d, –CH=); 24.9, 16.8 (2C, q, –CH_3); 31.8, 25.1, 22.1, 14.5 (8C, Sn–Bu^n). ^{119}Sn NMR ($CDCl_3$) δ (ppm): −243.8. IR (cm^{-1}): 1608 *v*(C = N); 1590, 1535 *v*(C=O); 675, 680 *v*(Sn–C); 529, 557, 575 *v*(Sn–O); 447 *v*(Sn–N). ESI-MS (*m/z*): 543.6.

2.4.4. [(n-Bu)$_2$Sn(o-smab)(ea)] (4)

Yield: 79%, Yellow solid, m.p. 119–121 °C, MW: 503.26; Elem. Anal. for $C_{24}H_{36}N_2O_2Sn$, Calcd: C, 57.28; H, 7.21; N, 5.57; Sn, 23.59. Found: C, 57.09; H, 7.01; N, 5.35; Sn, 23.10%. ^{1}H NMR ($CDCl_3$) δ (ppm): 9.61 (1H, s, CH= N; 7.95–6.85 (8H, m, Ar–H); 1.65–1.21 (12H, m, Sn–$(CH_2)_3$–); 0.88 (6H, t, CH_3); 2.34 (3H, s, Ar–CH_3); 3.36 (2H, t, O–CH_2–); 2.48 (2H, t, N–CH_2); 2.63(1H, NH_2). ^{13}C NMR ($CDCl_3$) δ (ppm): 163.2 (1C, CO) 158.3 (s, –**C**=N); 146.8, 139.1, 135.2, 133.8, 130.9, 129.0, 125.1, 124.9, 121.8, 118.5, 114.9 (11C, Ar–**C**); 46.9 (1C, –O–**C**H_2); 33.1 (1C, –N–**C**H_2); 29.0, 23.5, 19.5, 13.2 (8C, Sn–Bu^n). ^{119}Sn NMR ($CDCl_3$) δ (ppm): −248.4. IR (cm^{-1}): 1607 *v*(C = N); 642, 675 *v*(Sn–C); 530, 548 *v*(Sn–O); 454, 429 *v*(Sn–N). ESI-MS (*m/z*): 502.9.

2.4.5. [(n-Bu)$_2$Sn(p-smab)(acac)] (5)

Yield: 74%, dark yellow solid, m.p. 115–118 °C, MW: 544.31; Elem. Anal. for $C_{25}H_{38}N_2O_2Sn$, Calcd: C, 59.58; H, 7.22; N, 2.57; Sn, 21.81. Found: C, 59.12; H, 7.09; N, 2.41; Sn, 21.13%. ^{1}H NMR ($CDCl_3$) δ (ppm): 9.48 (1H, s, CH = N); 8.14–7.15 (8H, m, Ar–H); 1.59–1.21 (12H, m, Sn–$(CH_2)_3$–); 0.90 (6H, t, CH_3); 2.29 (3H, s, Ar–CH_3); 3.55 (2H, t, O–CH_2–); 2.49 (2H, t, N–CH_2); 2.45 (1H, NH_2). ^{13}C NMR ($CDCl_3$) δ (ppm): 163.0 (s, CO); 158.7 (1C, –C=N); 148.0, 141.5, 138.7, 135.4, 132.5, 129.4, 124.5, 120.7, 116.9, 115.6, 113.1 (11C, Ar–C); 188.9 (–C–O); 81.5 (1C, –CH=); 23.9, 16.2 (2C, –CH_3); 29.1, 24.5, 21.7, 14.8 (8C, Sn–Bu^n). ^{119}Sn NMR ($CDCl_3$) δ (ppm): −245.1. IR (cm^{-1}): 1610 *v*(C=N); 1568, 1531 *v*(C=O); 651, 675 *v*(Sn–C); 511, 529, 552 *v*(Sn–O); 424 *v*(Sn–N). ESI-MS (*m/z*): 543.9.

2.4.6. [(n-Bu)$_2$Sn(p-smab)(ea)] (6)

Yield: 71%, brown solid, m.p. 130–132 °C, MW: 503.26; Elem. Anal. for $C_{24}H_{36}N_2O_2Sn$, Calcd: C, 57.28; H, 7.21; N, 5.57; Sn, 23.59 Found: C, 57.10; H, 1.36; N, 7.45; Sn, 23.22%. ^{1}H NMR ($CDCl_3$) δ (ppm): 9.62 (1H, s, CH = N); 7.65–6.95 (8H, m, Ar); 1.69–1.30 (12H, m, Sn–$(CH_2)_3$–); 0.88 (6H, t, CH_3); 2.27 (3H, s, Ar–CH_3); 3.51 (2H, t, O–CH_2–); 2.56 (2H, br, N–CH_2); 2.39 (1H, NH_2). ^{13}C NMR ($CDCl_3$) δ (ppm): 159.2 (1C, CO); 157.9 (1C, –C=N); 146.8, 136.1, 135.9, 134.7, 131.3, 130.4, 123.3, 121.1, 114.9, 115.6 (11C, Ar–C); 45.3 (1C, –O–CH_2); 32.5 (1C, –N–CH_2); 27.7, 23.1, 20.9, 13.8 (8C, Sn–Bu^n). ^{19}Sn NMR ($CDCl_3$) δ (ppm): −246.9. IR (cm^{-1}): 1612 *v*(C=N); 651, 678 *v*(Sn–C); 559, 532 *v*(Sn–O); 449, 429 *v*(Sn–N). ESI-MS (*m/z*): 502.2.

3. Results and discussion

Complexes **1**–**6** have been synthesized by the reaction of N-arylsalicylaldiminate derivatives of di-*n*-butyltin(IV) chloride with sodium salts of mono-functional bidentate ligands in 1:1 ratio in THF-C_6H_6 mixture (Scheme 1). All these complexes are colored solids, soluble in polar solvents (e.g. methanol, ethanol, THF, DMF, and DMSO).

3.1. Infrared spectroscopy

The IR spectra of mixed-ligand complexes of di-*n*-butyltin(IV) dichloride provide useful information for assigning the coordination mode of Schiff bases and monofunctional bidentate ligands to the tin atom. Salient characteristic of IR spectra is the disappearance of stretching vibration bands in the region 3430–3458 cm^{-1} due to phenolic

(OH) group of Schiff bases which is consistent with metallation of phenolic hydrogen on complexation [15]. The strong and sharp bands characteristic of ν(C = N) in the region 1634–1616 cm^{-1} observed in the free Schiff base ligands were shifted to lower frequencies (~31–11 cm^{-1}) in complexes [18].

The disappearance of a band at 1680 cm^{-1} is due to ν(C=O) group of free acetylacetone and appearance of bands at 1583 ± 8 cm^{-1} and 1530 ± 10 cm^{-1} are assigned to ν(C ⋯ C) coupled with ν(C ⋯ O) and ν(C ⋯ O) coupled with ν(C ⋯ C), respectively, that is consistent with the involvement of C = O group in the chelate formation in **1**, **3**, and **5** [23, 24].

Free ethanolamine in the liquid state gives a strong band at 3340 cm^{-1}, which is attributed to the ν(O–H) mode while the two other bands appearing at 3290 and 3160 cm^{-1} are assigned to the asymmetric and symmetric N–H stretching modes, respectively. The disappearance of a band at 3340 cm^{-1} and shifting of N–H stretching frequencies in the lower frequency region in **2**, **4**, and **6** clearly indicates coordination of tin to the oxygen and nitrogen atom of the NH_2 group [25, 26].

The new strong to medium absorption bands appear in the range 510 ± 60 cm^{-1}, which should be assigned to the ν(Sn–O) stretching mode according to the literature [22–24]. The results prove that the hydroxyl group is deprotonated and coordinated to the central tin atom. Further appearance of medium intensity bands 430 ± 30 cm^{-1} and strong to medium absorption bands 690 ± 15 cm^{-1} were attributed to ν(Sn–N) and ν(Sn–C), respectively [22–26] (representative IR spectrum of **2** in Supplementary material Figure S1).

3.2. ^{1}H NMR spectral studies

^{1}H NMR spectra of **1**–**6** exhibit no signal due to phenolic O–H of Schiff bases in the region 13.25–12.75 ppm due to metallation of phenolic O–H. In the spectra of complexes slightly downward chemical shift values in the region 9.89–9.48 ppm for –C**H**=N– protons may arise due to participation of azomethine nitrogen in chelation compared to that of the parent Schiff bases in the region 9.23–8.23 ppm [19]. Complexes **1**, **3**, and **5** show signals in the region 2.07–1.94 ppm and 5.50–5.48 ppm due to methyl and methine protons of acetylacetonate moiety, indicating the bidentate bonding mode of acetylacetonate [24]. The absence of a signal at 5.41 ppm corresponding to O–H group of ethanolamine supports its coordination to tin atom via deprotonation in **2**, **4**, and **6** [26]. In **2**, **4**, and **6**, signals due to NH_2 group were observed in the region 2.54–2.53 ppm. The resonance signals in the range 3.63–3.59 ppm and 2.56–2.51 ppm were assigned to CH_2–O and CH_2–N protons of ethanolamine, respectively [25], in **2**, **4**, and **6**. The characteristic aromatic signatures in **1**–**6** were observed in the range 7.17–8.06 ppm. Additionally, **3**–**6** displayed a sharp signal at 1.19 ppm assigned to CH_3 protons (representative ^{1}H NMR spectrum of **2** in Supplementary material Figure S2).

3.3. ^{13}C NMR spectral studies

^{13}C NMR spectra of **1**–**6** exhibit signals due to azomethine carbon in the region 160.5–158.9 ppm, shifted downfield compared to that of parent Schiff bases

(158.3–156.5 ppm), indicating coordination of azomethine nitrogen to tin. Signals at 163.8–161.1 ppm support formation of Sn–O–C bond and deprotonation of phenolic group. In **1**, **3** and **5**, two signals for the carbonyl carbon atoms of the acetylacetonate moiety are observed in the region 190.31–189.55 ppm and two signals for the methyl carbon of acetylacetonate have also been observed in the region 25.76–25.38 ppm. The appearance of two signals each for carbonyl carbon and methyl carbon for **1**, **3**, and **5** supports the bidentate chelating nature of the acetylacetonate moiety [24]. In **2**, **4**, and **6**, signals due to the –**C**H_2–O and –**C**H_2–N appear slightly downfield region in the region 49.0–45.3 and 33.1–31.8 ppm, respectively, compared to free ethanolamine at 63.7 and 43.8 ppm, respectively, indicating bidentate coordinating mode of ethanolamine [27] (representative ^{13}C NMR spectrum of **2** in Supplementary material Figure S3).

3.4. ^{119}Sn NMR spectral studies

To provide further evidence to establish the structure of the complexes in solution, ^{119}Sn NMR spectra were recorded. It is well known that ^{119}Sn chemical shifts are very sensitive to changes in the coordination number of tin and to the nature of groups directly attached to the tin atom. Complexes **1**–**6** exhibit a single sharp ^{119}Sn resonance (see Experimental Section) in the region −243.8 to −248.4 ppm, revealing the six-coordinate geometry around tin atom [26] (representative ^{119}Sn NMR spectrum of **2** in Supplementary material Figure S4).

3.5. Mass spectral studies

The mass spectra of **1**–**6** exhibit molecular ion peaks (*m/z*) which correspond to the molecular composition of the complexes. In the mass spectra of complexes, most of the fragments were observed as group of peaks due to various isotopes of tin. One representative mass spectrum (Supplementary material Figure S5) and its fragmentation pattern [16–18] (Scheme 2) with *m/z* for **1**, [(*n*-Bu)$_2$(sap)(acac)], has been suggested. In the spectrum of **1**, the molecular peak was observed at *m/z* 531.1 [calculated mass = 531.27]. The calculated isotopic distribution for molecular ion peak at *m/z* 531.2, 485.3, 467.3, and 425.3 for **1** are shown in Supplementary material Figure S6. The comparison of the calculated (bars) isotopic distribution for molecular ion peak and other important peaks with the mass spectrum of **1** confirms the molecular composition of the complex.

3.6. Computational studies

Since we were unable to grow suitable single-crystal for X-ray studies, computational method has been incorporated to derive properties of the molecule based on a determination of the electron density of the molecule. DFT calculations were carried out for the ligands and their complexes in gas phase to fully optimize the ground state structure. Molecular structure of ligand and organotin(IV) complex with atom labeling scheme is

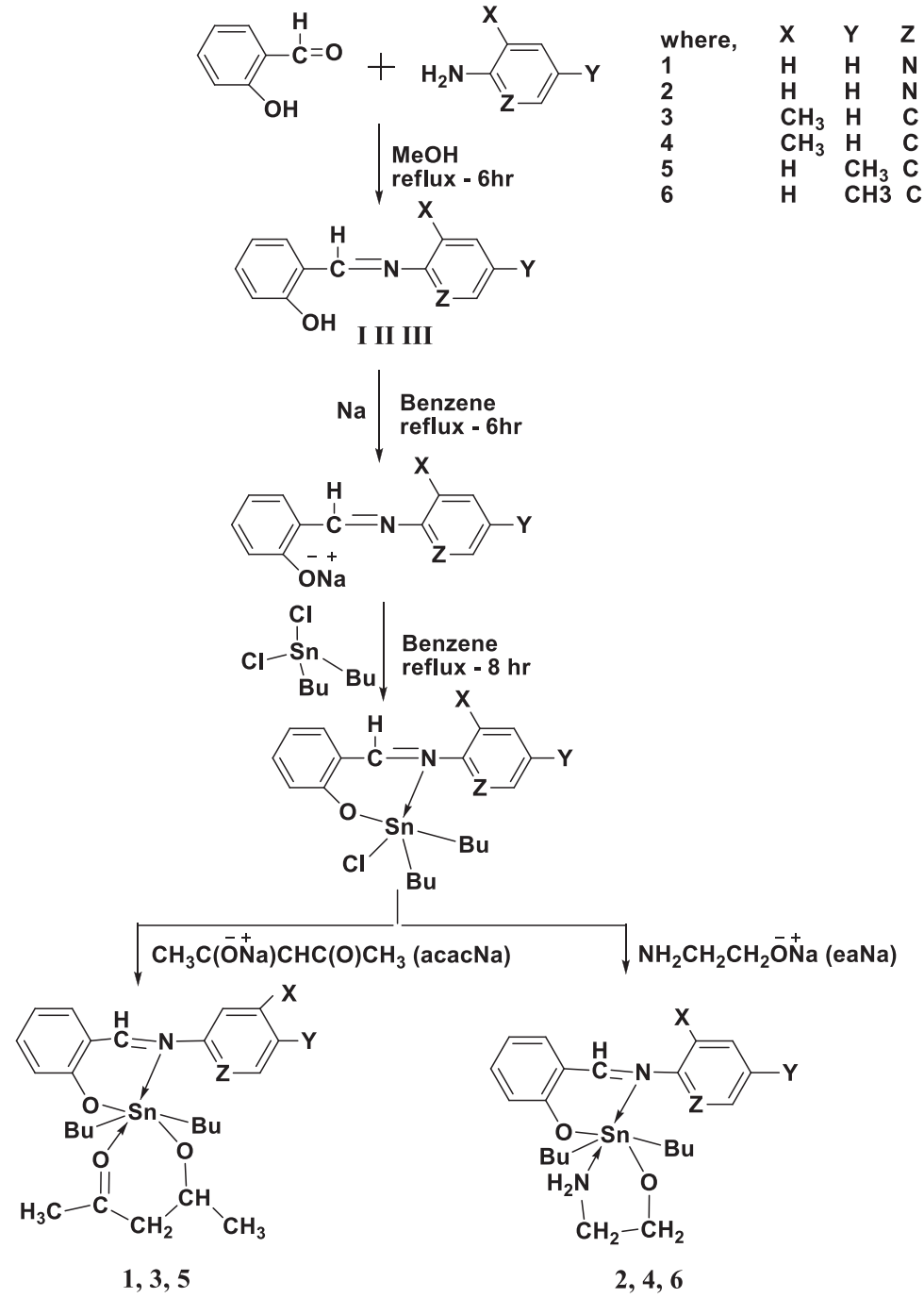

Scheme 1. Synthetic route for the preparation of mixed-ligand diorganotin complexes.

shown in Figure 1 and selected bond lengths and angles are summarized in Table 1. The optimized energy, dipole moment and energy band gap values are summarized in Table 2.

The theoretically calculated values of different bond lengths (Sn–O, Sn←O, Sn–C, Sn–N and Sn←N) in complexes are in close agreement to the values reported [28, 29]

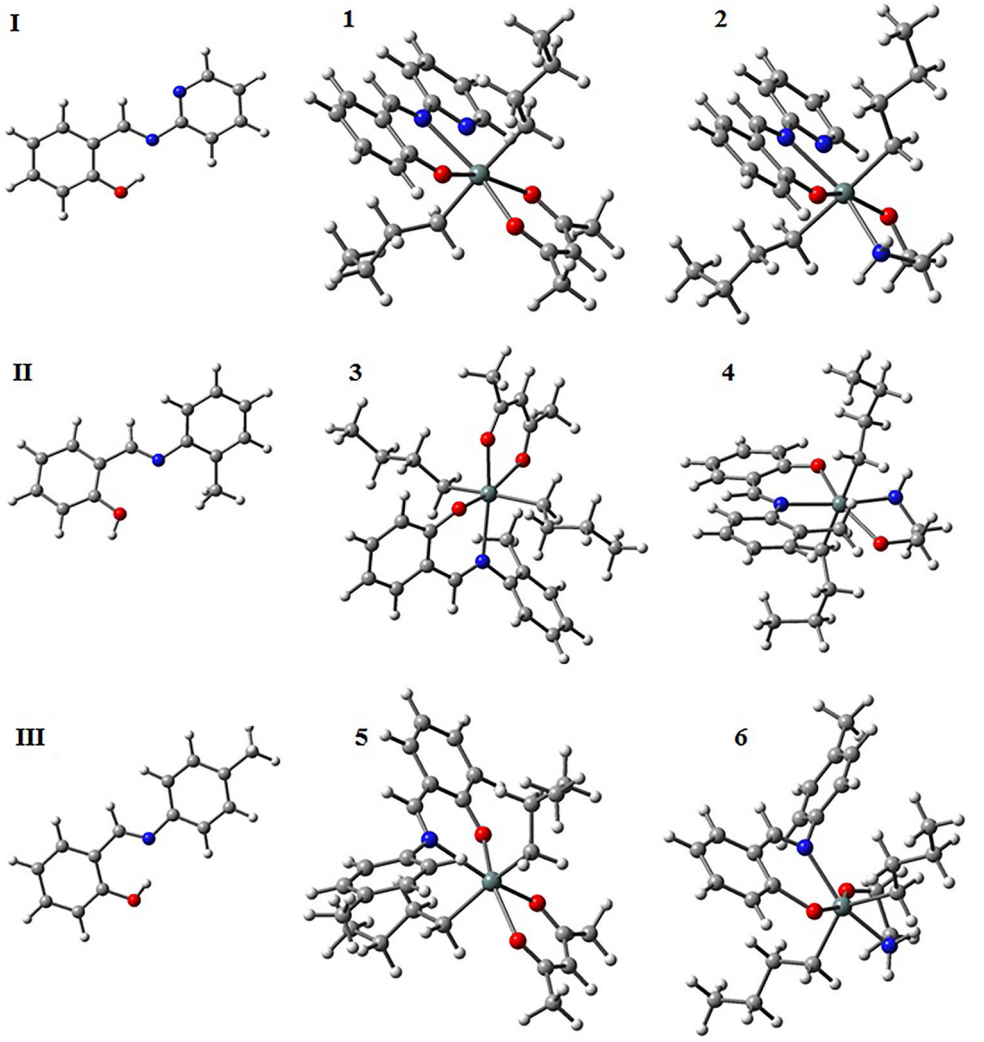

Figure 1. The ground state optimized geometry for ligands (**I-III**) and complexes (**1**–**6**) at B3LYP/LANL2DZ level.

for diorganotin(IV) complexes of N,O-donor ligands in distorted octahedral system. In all complexes, the axial positions to the Sn atom are occupied by two *n*-butyl group while the four equatorial positions to the Sn atom are engaged with N,O-donor Schiff base and mono-functional bidentate ligands [11, 29]. In **1**, **3**, and **5**, the presence of one phenolate and acetylacetonate ion as a result of deprotonation of Schiff base (LH) and mono-functional bidentate ligands acetylacetone (acacH) indicates covalent bonding *via* Sn–O(22) and Sn–O(26) and coordinate bonding through Sn←N(20) and Sn←O(25). Similarly in **2**, **4** and **6**, mono-functional bidentate ligand ethanolamine renders bonding through Sn–O(22), Sn–O(25) covalent and Sn←N(20), Sn←N(53) coordinate mode. The value of the Sn–O distance, in the range 2.04–2.30 Å and Sn–N distance in the range 2.47–2.37 Å as well as the other bond distances and angle are in good

Table 1. Selected structural parameters for [(n-Bu)$_2$Sn(sap)(acac)] and [(*n*-Bu)$_2$Sn(sap)(en)] at B3LYP/LanL2DZ level of theory.

Bond length (A°) [(*n*-Bu)$_2$Sn(sap)(acac)]		Bond angle (°) [(*n*-Bu)$_2$Sn(sap)(acac)]	
Sn-N20	2.47795	C43-Sn-N20	88.57330
Sn-O22	2.04253	O22-Sn-N20	74.52955
Sn-O25	2.30459	O22-Sn-C40	97.86648
Sn-O26	2.10504	C40-Sn-O26	94.38568
Sn-C40	2.13154	O26-Sn-O25	76.33859
Sn-C43	2.13226	O25-Sn-C43	83.67905
C11-N20	1.39970	Sn-O25-C30	132.7432
C19=N20	1.28340	Sn-O26-C31	138.6650
C2-O22	1.30822	Sn-C43-C56	116.3626
C31-O26	1.28497	Sn-C40-C46	116.6345
O25=C30	1.26938	Sn-N20-C19	129.2021
		Sn-O22-C2	144.8220
		Sn-N20-C11	105.3988
Bond length (A°) [(*n*-Bu)$_2$Sn(sap)(ea)]		Bond angle (°) [(*n*-Bu)$_2$Sn(sap)(ea)]	
Sn-N20	2.42890	C27-Sn-C30	178.2605
Sn-N53	2.37778	C27-Sn-N20	91.4404
Sn-O22	2.25885	C27-Sn-N20	91.4404
Sn-O25	2.08783	C27-Sn-N53	91.9699
Sn-C27	2.16600	C30-Sn-N20	86.9436
Sn-C30	2.17188	C30-Sn-N53	89.7361
		C27-Sn-O25	89.4851
		C27-Sn-O22	88.2459
		C30-Sn-O25	91.2453
		C30-Sn-O22	91.91362
		O22-Sn-N53	73.61931
		O25-Sn-N53	76.3533
		O25-Sn-N20	136.5452
		O22-Sn-N20	73.6462

Table 2. The computed electronic properties for ligands and complexes.

Complex	Total energy	DM	HOMO	LUMO	HOMO-LUMO gap
sapH (**I**)	−648.192	1.845	−0.2240	−0.0799	0.1441
[(*n*-Bu)$_2$Sn(sap)(acac)] (**1**)	−1302.408	4.650	−0.2794	−0.0561	0.2233
[(*n*-Bu)$_2$Sn(sap)(ea)] (**2**)	−1168.19	9.909	−0.2895	−0.0661	0.2234
o-smabH (**II**)	−671.30	2.608	−0.2049	−0.0501	0.1548
[(*n*-Bu)$_2$Sn(*o*-smab)(acac)] (**3**)	−1334.71	1.5565	−0.2065	−0.0639	0.1417
[(*n*-Bu)$_2$Sn(*o*-smab)(ea)] (**4**)	−1191.16	2.680	0.2857	−0.0611	0.2246
p-smabH (**III**)	−671.47	2.458	−0.2198	−0.0694	0.1504
[(*n*-Bu)$_2$Sn(*p*-smab)(acac)] (**5**)	−1325.84	2.1578	−0.2847	−0.0824	0.2023
[(*n*-Bu)$_2$Sn(*p*-smab)(ea)] (**6**)	−1191.25	2.3934	−0.2895	−0.0707	0.2188

agreement, for **1** and **2**, with the values reported for Sn–complexes using X-ray diffraction [11, 29]. The slight deviations in the values of bond angles from perfect octahedral geometry suggest distorted octahedral geometry around tin [7].

In order to know the stability of the complexes, energy gaps ($\Delta E = E_{LUMO} - E_{HOMO}$) of complexes have been calculated. The stability of the complexes is proportional to the energy band gap [15]. The highest occupied molecular orbital (HOMO) and the lowest unoccupied molecular orbital (LUMO) of ligand **I** and **1** and **2** are also shown in Figure 2. The comparison of total energy (E) and energy gap (ΔE) of ligands and complexes also suggest stability of complexes. The HOMO-LUMO energy gap of **1** and **2** (0.223 au/6.076 eV and 0.2234 au/6.078 eV, respectively) is higher than corresponding

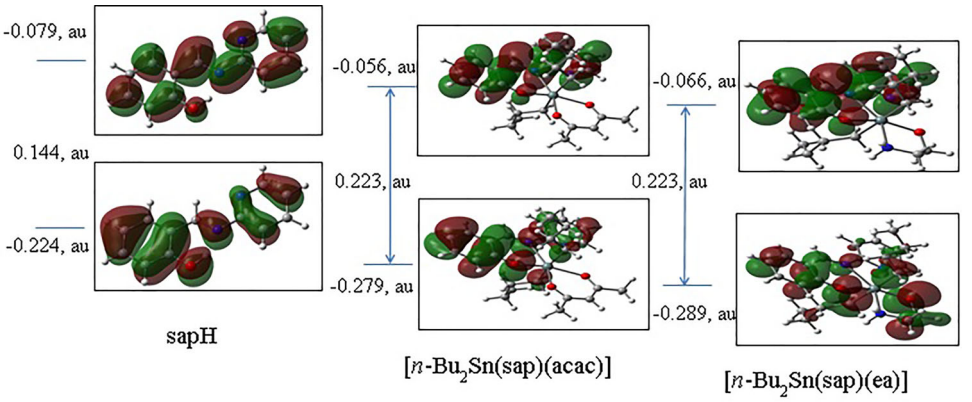

Figure 2. Energy diagram of frontier molecular orbitals HOMO and LUMO of ligand **I** and complexes **1** and **2** derived from DFT calculations using B3LYP/LANL2DZ level of theory.

ligand **I** (0.1441 au/3.921 eV). The obtained energy gap (ΔE) values of optimized complexes suggest the following order of stability, that is, **4** > **2** > **1** > **6** > **5** > **3**.

3.7. Thermal studies

The thermal stability of **1** and **2** was investigated through thermogravimetric analyses in the temperature range 30–600 °C at a heating rate of 10 °C/min under atmospheric conditions. The thermograms (Supplementary material Figure S7) of the mixed-ligand organotin complexes show decomposition during thermal analysis. The first step, at 30–180 °C, involves the loss of two butyl groups with mass loss of 21.2% (calculated mass loss 21.5%) and 22.9% (calculated mass loss 23.3%) for **1** and **2**, respectively. From 180–260 °C, loss of salicylidimanate moiety corresponds to mass loss of 58.5% (calculated mass loss 58.8%) and 63.1% (calculated mass loss 63.5%) for **1** and **2**, respectively. Further increase up to 600 °C gives final residue of SnO corresponding to 24.9%, which is in good agreement with calculated value of 25.3% for **1** and 26.5% compared to calculated value 27.4% for **2**.

3.8. In vitro antibacterial and antifungal activity of organotin complexes

The biological activity of the ligands **I**–**III** and organotin(IV) complexes **1**–**6** was carried out against different strain of bacteria such as *E. coli*, *S. aureus*, *P. aeruginosa*, *S. epidermidis* and fungi *A. niger*, *C. albicans*, *T. rubrum*, *Microsporum*. The diffusion agar technique was used to assess the antibacterial activity of the synthesized ligands and mixed-ligand organotin complexes. The antibacterial and antimicrobial activity data obtained for the ligands and organotin(IV) complexes are summarized in Tables 3 and 4.

Comparison of antimicrobial activities of organotin(IV) complexes **1**–**6** with the parent Schiff bases **I**–**III** showed that the organotin(IV) complexes displayed higher activity against the same microorganism compared to the parent Schiff base under identical experimental condition [30].

Table 3. Antibacterial activity[a] (diameter of inhibition zone) of Schiff bases and their mixed-ligand diorganotin(IV) derivatives.

	Inhibition zone diameter (mm)									
Bacterium	I	II	III	1	2	3	4	5	6	R[b]
E. coli	14 ± 0.32	6 ± 0.52	8 ± 0.13	17 ± 0.33	19 ± 0.28	15 ± 0.43	17 ± 0.28	14 ± 0.25	16 ± 0.32	22 ± 0.05
P. *aeruginosa*	13 ± 0.40	7 ± 0.41	9 ± 0.17	15 ± 0.28	18 ± 0.32	12 ± 0.26	14 ± 0.26	11 ± 0.28	13 ± 0.35	22 ± 0.07
S. aureus	17 ± 0.26	6 ± 0.48	7 ± 0.14	18 ± 0.36	19 ± 0.36	10 ± 0.37	16 ± 0.51	12 ± 0.29	15 ± 0.38	20 ± 0.08
S. epidermidis	9 ± 0.36	12 ± 0.38	13 ± 0.19	15 ± 0.30	15 ± 0.34	16 ± 0.29	19 ± 0.46	14 ± 0.31	18 ± 0.32	22 ± 0.07

[a]*In vitro*, agar well diffusion method, conc. 1 mg/mL in DMSO.
[b]R is reference drug, Tetracyclin.

Table 4. Antifungal activity[a] (diameter of inhibition zone) of Schiff bases and their mixed-ligand diorganotin(IV) derivatives.

	Inhibition zone diameter (mm)									
Bacterium	I	II	III	1	2	3	4	5	6	R[b]
A. niger	11 ± 0.26	12 ± 0.31	13 ± 0.30	14 ± 0.32	17 ± 0.29	15 ± 0.32	16 ± 0.34	15 ± 0.39	17 ± 0.37	23 ± 0.05
C. albicans	13 ± 0.21	9 ± 0.29	6 ± 0.32	15 ± 0.36	18 ± 0.27	13 ± 0.29	17 ± 0.36	13 ± 0.41	15 ± 0.38	23 ± 0.05
T. rubrum	7 ± 0.21	12 ± 0.28	8 ± 0.27	10 ± 0.34	13 ± 0.26	14 ± 0.27	18 ± 0.36	12 ± 0.38	16 ± 0.31	22 ± 0.06
Microsporum	9 ± 0.22	11 ± 0.21	14 ± 0.26	15 ± 0.31	19 ± 0.26	16 ± 0.25	19 ± 0.32	17 ± 0.40	20 ± 0.19	23 ± 0.05

[a]*In vitro*, agar well diffusion method, conc. 100 μg/mL in DMSO.
[b]R is reference drug, Fluconazole.

Complexes **1**–**6** have better antimicrobial activity than the parent Schiff base, which is due to the more lipophilic nature of complexes than the corresponding Schiff bases. The increased activity of organotin(IV) complexes can be explained on the basis of the chelation theory. Due to the polarity of the metal atom will be reduced to greater extent due to the overlap of the ligand orbital and partial sharing of positive charge of the metal atom with donor atoms. Furthermore, it also increases the delocalization of p-electrons over the whole chelate ring and enhance the lipophilicity enhanced the penetration of the complex into lipid membrane and blocks the metal binding sites on enzymes of micro-organisms and inhibit their multiplication [31].

4. Conclusion

Synthesis of six-coordinate di-*n*-butyltin(IV) complexes has been achieved by the reaction of [(*n*-Bu)2Sn(sb)Cl] with sodium salt of mono-functional bidentate ligands in 1:1 molar ratio and bidentate η^2-bonding nature of acetylacetone (acacH), ethanolamine (eaH) investigated by a variety of physicochemical methods. Molecular composition of the complexes is confirmed by the mass spectral studies. The DFT data also validate the results observed from the spectroscopic studies. The results of *in vitro* antimicrobial screening indicate that mixed-ligand *n*-butyltin(IV) complexes show moderate activity, which is also higher than that of the Schiff bases.

Acknowledgement

Authors gratefully acknowledge the CSIR and UGC for doctoral fellowship and Head, Department of Chemistry for providing laboratory facilities. Special thanks to SAIF Chandigarh for IR, NMR (^{1}H, ^{13}C, and ^{119}Sn) and Q-TOF LC-MS Mass spectra of the complexes and Head,

Department of Chemistry, Banaras Hindu University, Varanasi for ^{119}Sn spectra of the complexes and CDRI, Lucknow for providing elemental analysis.

Disclosure statement

No potential conflict of interest was reported by the authors.

References

[1] M. Roy, S. Roy, K.S. Singh, J. Kalita, S.S. Singh. *New J. Chem.*, **40**, 1471 (2016).
[2] C. Ma, Q. Wang, R. Zhang. *Inorg. Chem.*, **47**, 7060 (2008).
[3] C. Ma, Y. Han, R. Zhang, D. Wang. *Dalton Trans.*, **12**, 1832 (2004).
[4] M. Sirajuddin, S. Ali, V. McKee, S. Zaib, J. Iqbal. *RSC Adv.*, **4**, 57505 (2014).
[5] M.S. Ahmad, M. Hussain, M. Hanif, S. Ali, B. Mirza. *Molecules*, **12**, 2348 (2007).
[6] M. Hong, Y. Yang, C. Li, L. Xu, D. Li, C-z Li. *RSC Adv.*, **5**, 102885 (2015).
[7] Y.Y. Zhang, R.F. Zhang, S.L. Zhang, S. Cheng, Q.L. Lia, C.L. Ma. *Dalton Trans.*, **45**, 8412 (2016).
[8] G.M. Treich, S. Nasreen, A.M. Kanakkithodi, R. Ma, M. Tefferi, J. Flynn, Y. Cao, R. Ramprasad, G.A. Sotzing. *ACS Appl. Mater. Interfaces*, **8**, 21270 (2016).
[9] Q. Li, M.F.C.G.D. Silva, A.J.L. Pombeiro. *Chem. Eur. J.*, **10**, 1456 (2004).
[10] M. Nath, P.K. Saini. *Dalton Trans.*, **40**, 7077 (2011).
[11] F.A. Shah, S. Sabir, K. Fatima, S. Ali, I. Qadri, C. Rizzoli. *Dalton Trans.*, **44**, 10467 (2015).
[12] S. Shujha, A. Shah, Z. Rehman, N. Muhammada, S. Ali, R. Qureshi, N. Khalid, A. Meetsma. *Eur. J. Med. Chem.*, **45**, 2902 (2010).
[13] M. Hong, G. Chang, R. Li, M. Niu. *New J. Chem.*, **40**, 7889 (2016).
[14] T.S.B. Baul, P. Kehie, A. Duthie, N. Guchhait, N. Raviprakash, R.B. Mokhamatam, S.K. Manna, N. Armata, M. Scopelliti, R. Wang, U. Englert. *J. Inorg. Biochem.*, **168**, 76 (2017).
[15] M.N. Mridula. *J. Photochem. Photobiol. B*, **162**, 348 (2016).
[16] R.K. Dubey, A.P. Singh, S.A. Patil. *Inorg. Chim. Acta*, **410**, 39 (2014).
[17] R.K. Dubey, A.P. Singh. *J. Coord. Chem.*, **66**, 2201 (2013).
[18] (a) R.K. Dubey, A.P. Singh, N. Dwivedi. *Main Group Met. Chem.*, **34**, 77 (2011); (b) T.A.K. Al-Allaf, L.J. Rashan, A. Stelzner, D.R. Powell. *Appl. Organomet. Chem.*, **17**, 891 (2003).
[19] (a) R.K. Dubey, A.P. Singh, N. Dwivedi. *Phosphorus, Sulfur, Silicon Relat. Elem.*, **187**, 1038 (2012); (b) A.K. Kushwaha, Meenakshi, N. Jaiswal, A.P. Singh, R.K. Dubey. *Main Group Met. Chem.*, **40**, 41 (2017); (c) N. Sharma, V. Sharma, R. Bohra, V.S. Raju, I.P. Lorenz, C. Krinninger, P. Mayer. *Inorg. Chem. Acta*, **360**, 3002 (2007); (d) O.V. Makrova, T. Rajh, M.C. Thurnaure, A. Martin, P.A. Kemme, D. Cropek. *Environ. Sci. Technol.*, **34**, 4797 (2000); (e) A.S. Attar, M.S. Ghamsari, F. Hajiesmaeilbaigi, S. Mirdamadi. *J. Mater. Sci.*, **43**, 1723 (2008).
[20] (a) W.L.F. Armarego, D.D. Perrin, *Purification of Laboratory Chemicals*, 4th Edn, Butterworth, Henemann, Oxford (1997); (b) A.I. Vogel. *A Textbook of Quantitative Chemical Analysis*, 6th Edn, Longman Publisher, Harlow, UK (2006).
[21] (a) M.J. Frisch, G.W. Trucks, H.B. Schlegel, G.E. Scuseria, M.A. Robb, J.R. Cheeseman, G. Scalmani, V. Barone, B. Mennucci, G.A. Petersson, H. Nakatsuji, M. Caricato, X. Li, H.P. Hratchian, A.F. Izmaylov, J. Bloino, G. Zheng, J.L. Sonnenberg, M. Hada, M. Ehara, K. Toyota, R. Fukuda, J. Hasegawa, M. Ishida, T. Nakajima, Y. Honda, O. Kitao, H. Nakai, T. Vreven, J.A. Montgomery Jr., J.E. Peralta, F. Ogliaro, M. Bearpark, J.J. Heyd, E. Brothers, K.N. Kudin, V.N. Staroverov, R. Kobayashi, J. Normand, K. Raghavachari, A. Rendell, J.C. Burant, S.S. Iyengar, J. Tomasi, M. Cossi, N. Rega, J.M. Millam, M. Klene, J.E. Knox, J.B. Cross, V. Bakken, C. Adamo, J. Jaramillo, R. Gomperts, R.E. Stratmann, O. Yazyev, A.J. Austin, R. Cammi, C. Pomelli, J.W. Ochterski, R.L. Martin, K. Morokuma, V.G. Zakrzewski, G.A. Voth, P. Salvador, J.J. Dannenberg, S. Dapprich, A.D. Daniels, Ö. Farkas, J.B. Foresman, J.V. Ortiz, J. Cioslowski, D.J. Fox, *Gaussian 09 (Revision A.02)*, Gaussian, Inc., Wallingford, CT

(2009); (b) A.D. Becke. *J. Chem. Phys.*, **98**, 5648 (1993); (c) C. Lee, W. Yang, R.G. Parr. *Phys. Rev. B*, **37**, 785 (1988); (d) P.J. Hay, W.R. Wadt. *J. Chem. Phys.*, **82**, 299 (1985); (e) G.A. Miller, E.O. Schlemper. *Inorg. Chem.*, **12**, 677 (1973).

[22] M. Balouiri, M. Sadiki, S.K. Ibnsouda. *J. Pharm. Anal.*, **6**, 71 (2016).

[23] S.P. Narula, S. Kaur, R. Shankar, S. Verma, P. Venugopalan, S.K. Sharma, R.K. Chadha. *Inorg. Chem.*, **38**, 4777 (1999).

[24] C. Pettinari, F. Marchetti, A. Cingolani, D. Leonesi, E. Mundorff, M. Rossi, F. Caruso. *J. Organomet. Chem.*, **557**, 187 (1998).

[25] F. Arjmand, I. Yousuf. *J. Organomet. Chem.*, **743**, 55 (2013).

[26] (a) R.A. Khan, S. Yadav, Z. Hussain, F. Arjmanda, S. Tabassum. *Dalton Trans.*, **43**, 2534 (2014); (b) W.F. Howard Jr., R.W. Crecely, W.H. Nelson. *Inorg. Chem.*, **24**, 2204 (1985); (c) H. Holecek, M. Nadvornik, K. Handlir. *J. Organomet. Chem*., **315**, 299 (1986); (d) J. Otera. *J. Organomet. Chem.*, **221**, 57 (1981); (e) J. Otera, A. Kushaba, T. Hinoishi. *J. Organomet. Chem.*, **228**, 223 (1982).

[27] V.T. Yilmaz, Y. Topcu, F. Yilmaz, C. Thoene. *Polyhedron*, **20**, 3209 (2001).

[28] M.A. Salam, M.A. Hussein, I. Ramli, M.S. Islam. *J. Organomet. Chem.*, **813**, 71 (2016).

[29] E.L. Torres, F. Zani, M.A. Mendiola. *J. Inorg. Biochem.*, **105**, 600 (2011).

[30] W. Rehman, R. Yasmeen, F. Rahim, M. Waseem, C.-Y. Guo, Z. Hassan, U. Rashid, K. Ayub. *J. Photochem. Photobiol. B*, **164**, 65 (2016).

[31] T.S.B. Baul. *Appl. Organomet. Chem.*, **22**, 195 (2008).